Diffuse phase transition and magnetic-domain microstructures in a Cr-doped manganite thin film

Hirotaka Oshima,[1,2] Yasushige Ishihara,[1] Masao Nakamura,[1] and Kenjiro Miyano[1,2]
[1]*Department of Applied Physics, University of Tokyo, Bunkyo-ku, Tokyo 113-8656, Japan*
[2]*Japan Science and Technology Corporation (JST), Tokyo 171-0031, Japan*
(Received 12 June 2000; revised manuscript received 25 September 2000; published 12 February 2001)

Diffuse phase transition in a thin film of Cr-doped $Pr_{0.5}Ca_{0.5}MnO_3$ has been studied in both macroscopic and microscopic properties. Diffuse changes of the resistivity and magnetization and the glassy magnetic properties of the film suggest ferromagnetic regions of finite sizes. Images of magnetic microstructures of the film have been observed with a magnetic force microscope from room temperature to 40 K. The structure consists of a wide variety of length scales: structure of different length scale responding to the applied magnetic field differently. The behavior is consistent with the idea that Cr acts as a local random field resulting in the slow relaxation in diffuse phase transition as in the case of relaxor ferroelectrics.

DOI: 10.1103/PhysRevB.63.094420 PACS number(s): 75.30.Vn, 75.50.Lk, 75.70.Kw, 72.80.Ga

I. INTRODUCTION

In the hole-doped perovskite manganites, the strong coupling of the spin, charge, and orbital degrees of freedom leads to the nearly degenerate localized and itinerant electronic states. Offering opportunities for phase control and their applications, those systems have in the past ten years attracted considerable attention.[1] Particularly, recent researches[2,3] have revealed that coexistence of the insulating and conducting states plays a crucial role in determining the overall macroscopic transport properties. Therefore, microscopic study is indispensable for better understanding the origin of the macroscopic properties. This is especially true for the study of magnetic properties[4] in which the domain structure and its behavior under external field is the basic ingredients for interpreting the magnetization curve and for designing the magnetic recording media.

Due to the small average size of the Pr^{3+} and Ca^{2+} cations, hole-doped perovskite manganites $Pr_{1-x}Ca_xMnO_3$ remain insulating for the entire range of x.[5,6] The ferromagnetic-metallic (FM) state by the double-exchange mechanism[7] is suppressed by the charge-orbital order and the electron-lattice coupling because of the small transfer integral between Mn sites. Charge-orbital ordered (CO-OO) state in $Pr_{1-x}Ca_xMnO_3$ is most stabilized when $x=0.5$, the commensurate value for the formation of 1:1 Mn^{3+}/Mn^{4+} arrangement.[6] The insulating state, however, can be transformed into metallic state by external stimuli;[6,8–10] the transition by a magnetic field is called colossal magnetoresistance (CMR).

Recently, it has been shown that the small amount of *B*-site substitution with Cr also results in the CO-OO to FM transition.[11] It is qualitatively understood in terms of the random field effect[12,13] due to the Cr^{3+} ions which fix the local phase of the CO-OO state due to the e_g orbital deficiency. The term relaxor ferromagnet[14] coined to describe the phenomena in analogy with the relaxor ferroelectric[15] seems to be appropriate, although the situation is more complex in that the frustration between the out-of-phase domains does not lead to the high-temperature random phase (paramagnetic insulator) but leads to another ground state (FM). The relaxor behavior has been clearly demonstrated in Cr-doped $Nd_{0.5}Ca_{0.5}MnO_3$ (Refs. 14, 16) which is found to be phase separated in the form of FM clusters in a CO-OO insulating matrix. For example, an aging effect in which the magnetization and conductance increase slowly in a magnetic field at low temperature and magnetic-field-annealing of the magnetic and transport properties has been observed.[14] The physics of the relaxor system is important for the phase-control between the CO-OO AF and FM phases. For this purpose, the knowledge of magnetic-domain structures and spatio-temporal distribution of the FM phase, and their relation to the experimental variables (temperature, applied field, etc.) are essential. Especially, the length scale of the resulting domain structure [the Fukuyama-Lee-Rice length in a similar random field effect in the charge-density-wave (CDW) system[17]] should provide a clue to the nature of the random field.

In this article we present macroscopic and microscopic study on the magnetic properties of a $Pr_{0.5}Ca_{0.5}Mn_{0.96}Cr_{0.04}O_3$ thin film. To investigate the magnetic properties of the system, we have chosen a sample in thin film form, the surface flatness of which is suitable for the detection of magnetic-domain structures with a magnetic force microscope (MFM) in a submicrometer scale. Thin film form also facilitates optical measurements for further study of the system and is necessary when application for devices is taken into account. A diffuse phase transition and glassy magnetic properties of the film are shown. We then exhibit magnetic microstructures of the film and delayed and slow variation of the patterns using a home-built low-temperature MFM. It is revealed that even in a microscopic scale, inversion of the magnetization occurs slowly; fine random domain structures appear after reversal of the applied field and then are smoothed by cumulative field effect. The behavior observed here is consistent with the macroscopic relaxor behavior. It is rather different from that of a typical broad-band FM manganite.

II. THIN FILM SAMPLE

We prepared a $Pr_{0.5}Ca_{0.5}Mn_{0.96}Cr_{0.04}O_3$ film with thickness of 350 nm on a MgO (001) substrate by pulsed-laser

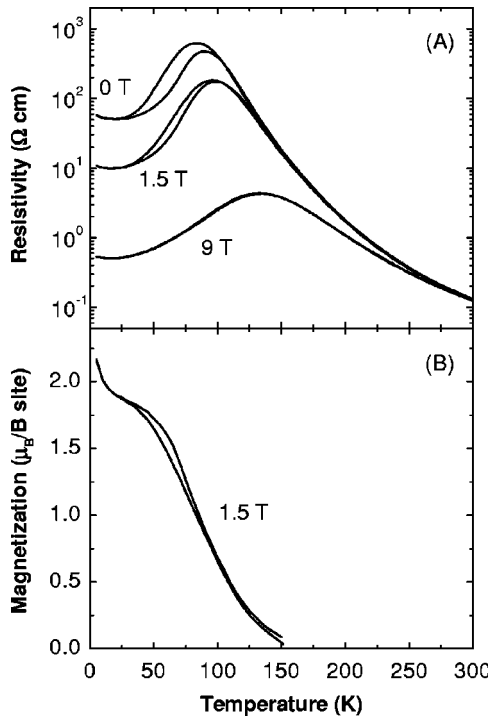

FIG. 1. (A) Temperature dependence of the resistivity under 0, 1.5, and 9 T for $Pr_{0.5}Ca_{0.5}Mn_{0.96}Cr_{0.04}O_3$ thin film on MgO (001) substrate. (B) Temperature dependence of the magnetization under 1.5 T for the same sample measured from 150 to 5 K and back to 150 K.

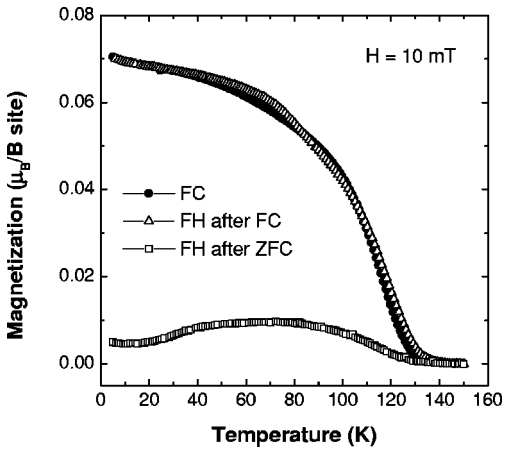

FIG. 2. Temperature dependence of the magnetization under 10 mT of the field in the cooling run (FC), the heating run after zero-field-cooling run (FH after ZFC), and the heating run after 10 mT field-cooling run (FH after FC).

deposition (PLD). For the target, stoichiometric mixtures of Pr_2O_3, $CaCO_3$, Mn_3O_4, and Cr_2O_3 were ground, calcined at 1000 °C for 14 h, ground again, pressed into a pellet of ϕ 20 mm×4 mm, and sintered at 1400 °C for 24 h in air. A substrate was held at 800 °C in an atmosphere of 1 mTorr oxygen during deposition. ArF excimer laser pulses of about 100 mJ with a repetition rate of 10 Hz were focused onto the target. After deposition, the film was annealed for 30 minutes at 700 °C and then cooled to room temperature in an hour in a 760 Torr oxygen atmosphere. X-ray diffraction indicated that the film was polycrystalline partially oriented with pseudocubic (001) and (011) along the film normal. The substrate inflicts little stress effect upon the sample.

III. RESISTIVITY AND MAGNETIZATION

Figure 1 shows (A) resistivity in magnetic field measured by four-probe method and (B) magnetization in 1.5 T of the field with a superconducting quantum interference device (SQUID) both as a function of temperature. The sample shows a broad resistivity peak characteristic of a diffuse insulator-metal (IM) transition as temperature decreases, and a gradual increase in the magnetization in the temperature region where the resistivity decreases. From these results, the diffuse appearance of a FM state over wide temperature range is confirmed. On applying magnetic field, the sample exhibits CMR effect. It is to be noted that the CMR effect occurs over broad range of temperature (even at the lowest temperature) and not only near the resistivity peak. Magnetization curves at 1.5 T [Fig. 1(B)] were measured in cooling and heating between 150 K and 5 K. The changes of the resistivity and magnetization are rather gradual, and the transition is at lower temperature than those of the bulk sample.[11] The difference is possibly due to oxygen stoichiometry, existence of the substrate which prevents the lattice constant change associated with the IM transition, or dimensionality of percolative behavior in the system. However, we suggest that the behavior of the transitions and CMR, and large residual resistance and relatively low value of magnetization in the FM state, are all consistent with the diffuse phase transition and phase separation.

Measurements of magnetization after zero-field-cooling (ZFC) and field-cooling (FC) runs respectively show completely different results (Fig. 2) as is the case for the spin glass materials. The magnetization measured in a field-heating (FH) run under 10 mT of the field after the ZFC run is much smaller than that measured in the same condition after the 10 mT-FC run. The reversibility of the FC/FH curves is also shown in Fig. 2. The difference between ZFC and FC measurement is not due to the change of the volume fraction of the FM regions by the magnetic field, but probably due to the freezing of the magnetization of the FM clusters. This view is justified from the result of the resistivity measurement as a function of temperature under 0 and 10 mT which showed identical values in both cooling and heating runs. We have also observed an extremely slow relaxation of the magnetization (~5% increase in 30 min) after the field application on the ZFC sample; a distinctive feature of the relaxor. The magnetization was measured only when the relaxation slowed down after several tens of minutes.

The frozen magnetization of the FM clusters is also seen in the magnetic hysteresis loop. In Fig. 3, magnetization versus magnetic field plot at 5 K after ZFC is shown. The first magnetization curve is lower than the curves taken afterward and out of the hysteresis loop, being consistent with the ZFC/FC experiments.

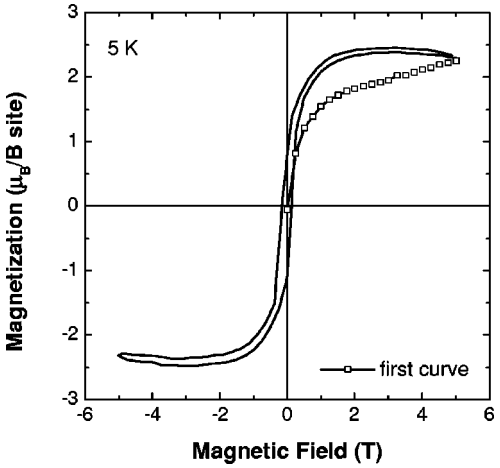

FIG. 3. Magnetic hysteresis loop at 5 K after the zero-field-cooling run.

IV. MAGNETIC FORCE MICROSCOPY

Our MFM measurements were carried out in frequency-modulation detection mode.[18] The magnetic field gradient $\partial B/\partial z$, where z is taken along the film normal, is detected as a shift of the resonance frequency of an oscillating magnetized cantilever, from which the magnetization pattern is visualized. It takes about 5 minutes to obtain an image reported here. The MFM is equipped with a small electromagnet capable of applying a magnetic field of up to 30 mT parallel to the sample. The duration of the field is limited to about 1 s in order to avoid the heating of the coil that has an adverse effect to the temperature stability. The usual procedure to see the response of the magnetic domains is to apply the field for 1 s before each scan unless stated otherwise.

The probe tip is coated with a magnetic thin film, which is magnetized axially due to the shape anisotropy. Using a magnetic recording disk, basic performance of the tip has been confirmed. (1) The reversal of the tip magnetization direction reverses the image contrast, hence the image is solely due to the sample magnetization. (2) The resolution is better than 50 nm. (3) The 30 mT field by the electromagnet, which is less than the coercive force of the disk, does not affect the image, hence the tip magnetization is unaltered. (4) The surface roughness of several nanometers does not show up in the MFM images because the tip is positioned tens of nanometers away.

The magnetic field from the tip is in general weak enough so that the images of the manganite films are reproducible after repeated scans. When the coercive force of the film is extremely small (as is the case shown in Fig. 7 below), the tip-induced magnetization noise is clearly seen.

The topographic images of the two film samples $Pr_{0.5}Ca_{0.5}Mn_{0.96}Cr_{0.04}O_3$ and $La_{0.6}Sr_{0.4}MnO_3$, measured with an atomic force microscope are shown in Fig. 4. A typical broad-band manganite $La_{0.6}Sr_{0.4}MnO_3$ was chosen as a reference to compare the MFM images, and will be discussed later. The patterns are similar in any regions of the samples. The root mean square of the surface roughness of the $Pr_{0.5}Ca_{0.5}Mn_{0.96}Cr_{0.04}O_3$ film is 1.0 nm (the maximum peak to valley depth is 8 nm), and the size of the observed pattern

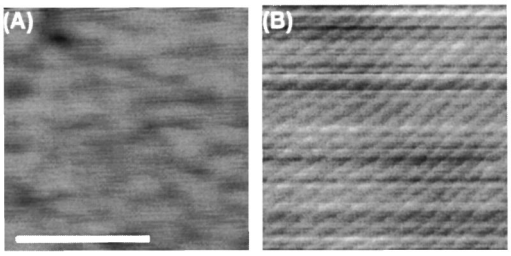

FIG. 4. Topographic images of (A) $Pr_{0.5}Ca_{0.5}Mn_{0.96}Cr_{0.04}O_3$ and (B) $La_{0.6}Sr_{0.4}MnO_3$ thin film samples. Images (A) and (B) are obtained over a 1.8 μm square; the white line in (A) indicate 1 μm. The maximum peak-to-peak roughness is 8 nm while its root mean square is 1.0 nm. Atomically flat terraces and steps are observed in (B). The steps are 0.4 nm high corresponding to a unit cell of the cubic perovskite structure.

is much smaller than 1 μm [Fig. 4(A)]. No distinct features as large as those of the MFM images shown below are observed. The $La_{0.6}Sr_{0.4}MnO_3$ thin film was epitaxially grown on a $SrTiO_3$ substrate and has atomically flat terraces separated by 0.4 nm-high steps corresponding to a unit cell length of the perovskite [Fig. 4(B)]. The step and terraces are also clearly different from the MFM images below. It is to be noted that the contrast in the MFM image roughly corresponds to 100 nm in the topological feature, if it were due to the surface roughness.

Because the MFM is sensitive to $\partial B/\partial z$, the image interpretation is always troublesome. It has been shown, for example, that for manganite films the MFM image tends to be diffuse when the magnetization lies in the film plane whereas clear domain boundaries are seen when the magnetization is along the film normal.[19] Our MFM images shown below all lack clear boundaries and thus seem to belong to the former category. On the other hand, the bubblelike appearance of our domain patterns resembles those observed in a layered-manganite with a Hall probe, in which the magnetization is along the film normal.[20] The normal magnetization seems to be more plausible when one considers that one cannot draw an arrow from a peak to a valley (or vise versa) in a manner consistent with the reversal of the applied field (shown below). Because more knowledge on the detail of the tip-sample interaction in the image-forming process is needed to settle the issue, we avert the question of the interpretation of the image in the present work. We instead use the MFM images simply as an indicator that delineates the extent of the uniformly magnetized region.

With this caveat in mind, we show MFM images of the magnetization pattern of the $Pr_{0.5}Ca_{0.5}Mn_{0.96}Cr_{0.04}O_3$ thin film at 95 K in Fig. 5. The temperature (95 K) is at the peak of the resistivity curve and in the middle of the gradual slope of the magnetization curve (Fig. 1); it is the temperature at which the FM domains are created in the insulating medium.

The time course of the experiment is illustrated at the bottom of the figures. The abscissa is the elapsed time and the tick marks indicate the magnetic field application ($\sim$1 s, 30 mT). The scanning (duration $\sim$5 min) was done every 5 min almost continuously except for the short

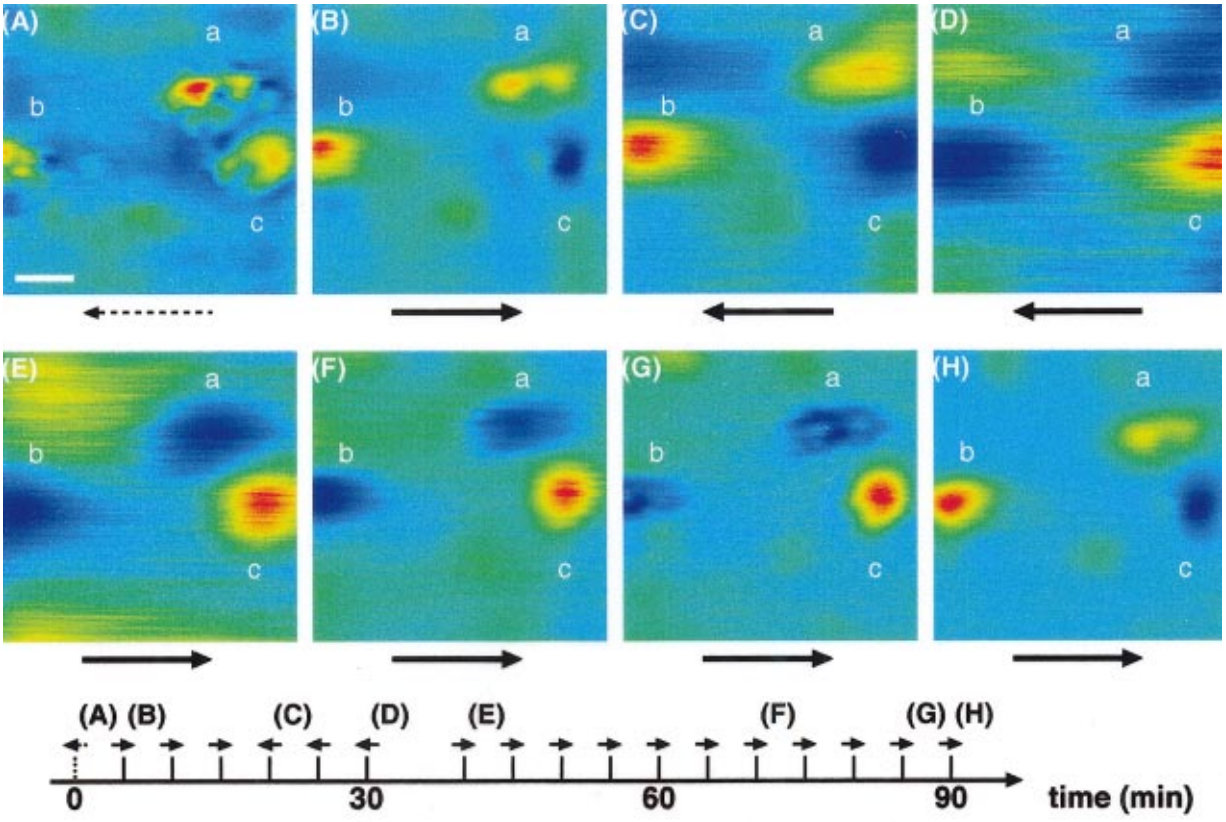

FIG. 5. (Color) Images of the magnetic microstructures of $Pr_{0.5}Ca_{0.5}Mn_{0.96}Cr_{0.04}O_3$ thin film sample at 95 K. Special attention is given to the structures marked as (a)–(c) showing delayed and slow relaxation. (A) With no field except the residual field. (B) After applying the field (30 mT). (C) After reversing the field. (D) Total delayed inversion of the domains. (E) After reversion of the field. (F) The sixth image after (E). (G) The appearance of internal fine structures signaling the commencement of the magnetization reversion. (H) Reversion of all the domains. All images are obtained over a 5 μm square. The white line in (A) indicates 1 μm. Solid arrows under the images indicate the directions of the applied field before each scanning. Dotted arrow in (A) indicates the direction of the residual field. Below the images, the time course of the experiment is shown; the field applications for about 1 s are denoted by the tick marks above which the directions of the field are shown. Each of the scans takes about 5 minutes after the field application.

intervals of the field application. The labels (A–H) indicate the corresponding images in the figures. The diagram thus shows that another frame was taken after (D) without the application of the field to insure the reproducibility. The first frame (A) was taken (after cooling down from the room temperature) without an applied field except for the residual field of about 1.5 mT from the core of the magnet.

There can be seen three distinguishable magnetic structures marked (a), (b), and (c). First, the magnetic field of 30 mT was applied from left to right [Fig. 5(B)] before the measurement. One can see the inversion of the spot (c) into blue, and the disappearance of the fine structures of the spots (a) and (b). This behavior of the spots indicates the inversion of the domain or the growth of the domains in their sizes. As the images showed no further change after two more field-applying and scanning runs, the direction of the applied field was reversed. In the first field-scan run, the image shown in Fig. 5(C) was obtained, which is not much different from Fig. 5(B). In the second run, the image remained unchanged. In the third run [Fig. 5(D)], however, colors of all the spots (a), (b), and (c) are reversed indicating the total inversion of the magnetic moment of those domain structures. The delayed relaxation of the magnetic-domain microstructures observed here is in accordance with the macroscopic relaxor behavior.

Next, we observed reappearance of the microstructures by switching the field at the same temperature. After the measurement of Fig. 5(D), the direction of the applied field was again reversed [Fig. 5(E)]. The repeated field application did not change the structures (a), (b), and (c) until we reached (F). Small spots in (a) and (b), together with the blue shadow in the left part of (c), appeared gradually in the images one of which is in Fig. 5(G). Finally, blue (a) and (b) turned into yellow and red, and red (c) with blue shadow on its left turned into blue with yellow shadow [Fig. 5(H)]. Here again, delayed and slow relaxation of magnetic-domain microstructures were seen clearly. It should be noted that Fig. 5(H) is quite similar to Fig. 5(B).

At a lower temperature (80 K), slower relaxation of the magnetic domain microstructure was observed as shown in Fig. 6. The sample was cooled to 80 K without the field. The first image [Fig. 6(A)] was taken after applying the magnetic field from right to left (in the opposite direction to that applied before cooling). Then, the direction of the field was

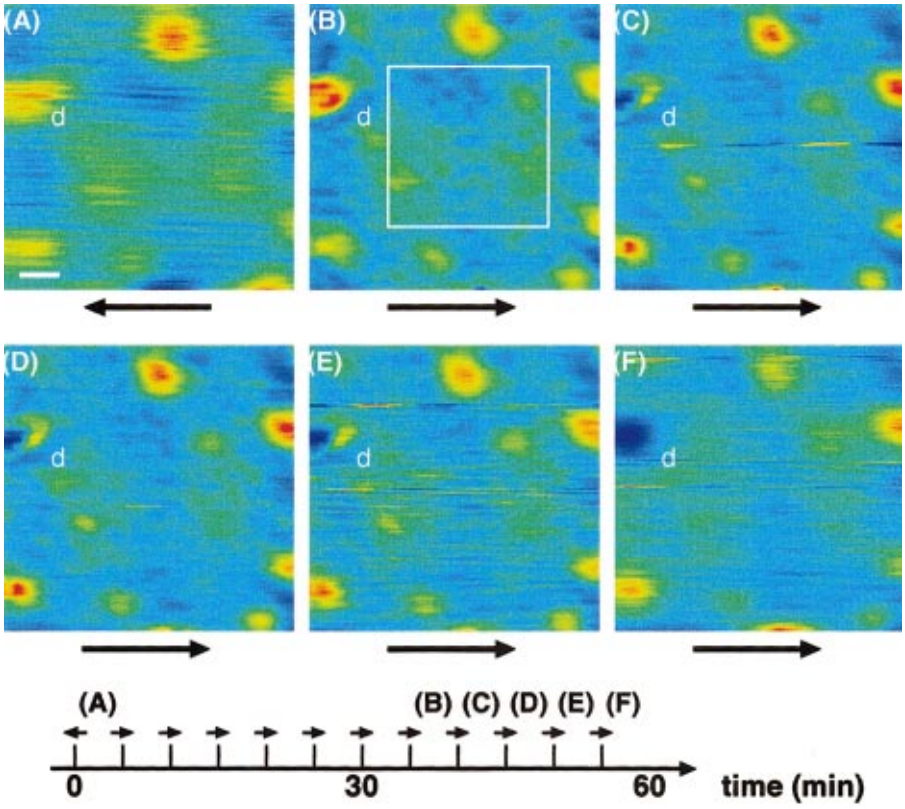

FIG. 6. (Color) Images of the magnetic microstructures of $Pr_{0.5}Ca_{0.5}Mn_{0.96}Cr_{0.04}O_3$ thin film sample at 80 K. The spot marked (d) shows slow relaxation. (A) After applying the field. (B) The seventh image after reversing the direction of the field. (C)–(F) From the eighth to eleventh images. The spot (d) reverses gradually. Images (A)–(F) are obtained over a 7 μm square. The white line in (A) indicates 1 μm. Arrows indicate the direction of the applied field. The white square in (B) indicates the area where frustrated disorder of the structures can be seen. Below the images, the time course of the experiment is shown; the field applications for about 1 s are denoted by the tick marks above which the directions of the field are shown. Each of the scans takes about 5 minutes after the field application.

reversed. Subsequently, seven images were taken applying the field before every scanning, but no distinctive change was observed up to the seventh one [Fig. 6(B)]. In the eighth image [Fig. 6(C)], there appeared blue part in the left of the spot marked (d). The blue area grew gradually and finally whole of the spot (d) turned into blue: Figs. 6(B)–6(F) represent five successive field/scan sequences. These figures clearly show the process of slow relaxation of the magnetic-domain microstructure. The behavior is slower than that at 95 K. At even lower temperature (40 K), we could not observe such inversion. The FM clusters were too stiff to be affected by the applied field of 30 mT, or the change was too sluggish. It is notable that these delayed relaxation shown above in Figs. 5 and 6 could be observed up to 126 K where there is only a little magnetization as seen in Fig. 1, and could not be detected at higher temperatures.

In addition to large spots as in (d), finer patterns are also discernible as depicted in the white square in Fig. 6(B). The finer patterns *appear* after the reversal of the applied magnetic field [as in (B)] but *disappear* after repeated applications of the field in one direction [as in (F)]. The tendency of frequent appearances of fine random structures in only some images after the inversion of the field was confirmed by repeated measurements. They are the frustrated magnetic domains with slow relaxation: the frustration is triggered by the field reversal but ''ironed out'' by the repeated application of the field. Closer inspection shows that the reversal of the spot (d) also involves the appearance of finer patterns in the intermediate states. Merging or smoothing down of the magnetic domains can sometimes be observed by application of a sequential magnetic field in disordered magnetic media as a consequence of the frustration induced by the domain wall pinning.[21] In this case the fine disordering of the domains is also caused by the frustration whose origin is probably the quenched random field. There are other spots in Fig. 6 that do not show complete magnetization reversal. The random coercive field distribution, frustration, and delayed response (even in the small magnetic domains) are all consistent with the microscopic relaxor behavior.

It should be added that, in Figs. 5 and 6, there exist unavoidable fine noises (horizontal dithering) probably due to extrinsic mechanical vibrations. Although Fig. 5(D) seems to be noisier than Fig. 5(A), for example, close numerical inspection shows that the amplitude of noise is in fact similar in both figures. The different appearance is only superficial. When the small scale features disappear [as in Fig. 5(D)], the

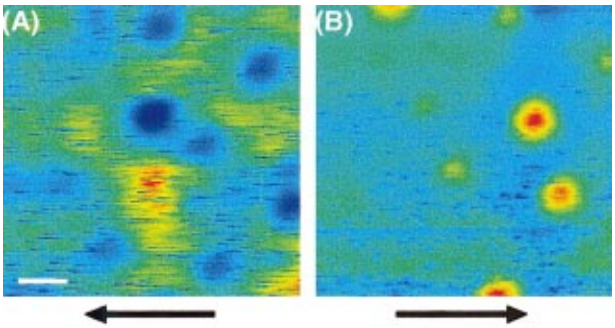

FIG. 7. (Color) Images of the magnetic microstructures of $La_{0.6}Sr_{0.4}MnO_3$ thin film sample at 120 K. (A) After applying the field. (B) After reversing the field. Further field application in the same direction does not change the pattern. The white line in (A) indicates 1 μm. Arrows indicate the direction of the applied field.

noise stands out clearly against the slowly changing featureless magnetization.

The difference between this sample and other FM manganites is important to understand the particular behavior of the sample. For reference, we fabricated an epitaxial $La_{0.6}Sr_{0.4}MnO_3$ thin film 100 nm thick on $SrTiO_3$ (001) substrate using the pulsed-laser deposition technique. $La_{0.6}Sr_{0.4}MnO_3$ is a typical broad-band FM manganite and our sample has a high T_C of 323 K and low coercive force (0.5 mT at 79 K). The MFM images taken at 120 K showed complete change of the magnetization pattern after one application of the reversing field (Fig. 7) and no further change after subsequent field application. However, the two patterns are not the negative of each other, which is probably due to the low coercive force of the sample and suggests that domains move more easily than the Cr-doped $Pr_{0.5}Ca_{0.5}MnO_3$ sample. Furthermore, many scratches are seen both in Figs. 7(A) and 7(B). They are probably due to the interactions between magnetization of the sample and the tip. As the coercive force of the sample is weak, sample magnetization can be influenced by the tip magnetization easily. Images of the $La_{0.6}Sr_{0.4}MnO_3$ film at room temperature, slightly lower than T_C, were also taken. Because of the weak magnetic moment of the sample at room temperature, however, the image was extremely faint. It is in contrast to the results of the Cr-doped $Pr_{0.5}Ca_{0.5}MnO_3$ sample which showed distinctive features even at the temperature above the resistivity peak. The contrasting behavior of the typical FM manganite attests peculiarity of the FM phase induced by the quenched random field in the Cr-doped system.

V. CONCLUSION

Diffuse phase change characteristic of relaxor systems has been observed in a thin film of a Cr-doped manganite in the temperature dependence of the resistivity and the magnetization. A low-temperature MFM reveals distributions of the magnetic field gradient perpendicular to the surface, hence the changes of magnetic structure in a wide range of temperature. Microscopic magnetic behavior consistent with the relaxor has been detected; delayed and slow inversion of magnetic domains together with the frustrated disordering of the domains in the diffuse phase transition region were clearly shown. It explains well the macroscopic glassy properties. The random impurity effect, which has been investigated especially in the CDW systems, high-temperature superconductors, and ferroelectrics, added a new way to the study of the CO-OO state in manganites as a local-field-induced global frustration in the coherent state of correlated electrons.

ACKNOWLEDGMENTS

We would like to thank H. Tamaru, Y. Taguchi, and M. Tokunaga for technical assistance. We are also grateful to M. Izumi, Y. Konishi, T. Manako, T. Kimura, M. Kawasaki, and Y. Tokura for valuable discussions and their help of our preparation of PLD apparatus and samples. We are indebted to Y. Otani for valuable comments. The work was supported in part by a Grant-in-Aid for COE Research from the Ministry of Education, Science, Sports and Culture, and by Japan Science and Technology Corporation (JST) through the CREST program.

[1] For a review, see, for instance, *Colossal Magnetoresistive Oxides*, edited by Y. Tokura (Gordon & Breach, New York, 1999).
[2] A. Moreo, S. Yunoki, and E. Dagotto, Science **283**, 2034 (1999).
[3] M. Uehara, S. Mori, C.H. Chen, and S.-W. Cheong, Nature (London) **399**, 560 (1999).
[4] U. Welp, A. Berger, D.J. Miller, V.K. Vlasko-Vlasov, K.E. Gray, and J.F. Mitchell, Phys. Rev. Lett. **83**, 4180 (1999).
[5] Z. Jirak, S. Krupicka, Z. Simsa, M. Dlouba, and S. Vratislav, J. Magn. Magn. Mater. **53**, 153 (1985).
[6] Y. Tomioka, A. Asamitsu, H. Kuwahara, Y. Moritomo, and Y. Tokura, Phys. Rev. B **53**, 1689 (1996).
[7] P.G. de Gennes, Phys. Rev. **118**, 141 (1960).
[8] A. Asamitsu, Y. Tomioka, H. Kuwahara, and Y. Tokura, Nature (London) **388**, 50 (1997).
[9] V. Kiryukhin, D. Casa, J.P. Hill, B. Keimer, A. Vigliante, Y. Tomioka, and Y. Tokura, Nature (London) **386**, 813 (1997).
[10] K. Miyano, T. Tanaka, Y. Tomioka, and Y. Tokura, Phys. Rev. Lett. **78**, 4257 (1997).
[11] B. Raveau, A. Maignan, and C. Martin, J. Solid State Chem. **130**, 162 (1997).
[12] Y. Imry and S.K. Ma, Phys. Rev. Lett. **35**, 1399 (1975).
[13] T. Katsufuji, S.-W. Cheong, S. Mori, and C.H. Chen, J. Phys. Soc. Jpn. **68**, 1090 (1999).
[14] T. Kimura, Y. Tomioka, R. Kumai, Y. Okimoto, and Y. Tokura, Phys. Rev. Lett. **83**, 3940 (1999).
[15] V. Westphal, W. Kleemann, and M.D. Glinchuk, Phys. Rev. Lett. **68**, 847 (1992).
[16] Y. Moritomo, A. Machida, S. Mori, N. Yamamoto, and A. Nakamura, Phys. Rev. B **60**, 9220 (1999).
[17] H. Fukuyama and P.A. Lee, Phys. Rev. B **17**, 535 (1978).
[18] T.R. Albrecht, P. Grütter, D. Horne, and D. Rugar, J. Appl. Phys. **69**, 668 (1991).
[19] C. Kwon, S.E. Lofland, S.M. Bhagat, M. Rajeswari, T. Venkatesan, R. Ramesh, A.R. Kratz, and R.D. Gomez, IEEE Trans. Magn. **33**, 3964 (1997).
[20] T. Fukumura, H. Sugawara, T. Hasegawa, K. Tanaka, H. Sakaki, T. Kimura, and Y. Tokura, Science **284**, 1969 (1999).
[21] B. Barbara, B. Dieny, and J. Filippi, J. Appl. Phys. **67**, 5763 (1990).